Chinese Chemical Letters 31 (2020) 172–176

Contents lists available at ScienceDirect

Chinese Chemical Letters

journal homepage: www.elsevier.com/locate/cclet

Communication

A designed locked nucleic acid-based nanopore for discriminating ctDNA and its coexisting analogue ncDNA

Yuqin Huang[a], You Lv[a], Jia Geng[b], Dan Xiao[a], Cuisong Zhou[a,*]

[a] College of Chemistry, Sichuan University, Chengdu 610064, China
[b] Department of Laboratory Medicine, State Key Laboratory of Biotherapy, West China Hospital, Sichuan University and Collaborative Innovation Center for Biotherapy, Chengdu 610041, China

ARTICLE INFO

Article history:
Received 15 April 2019
Received in revised form 16 May 2019
Accepted 17 May 2019
Available online 19 May 2019

Keywords:
Single-base difference
Simultaneous discrimination
Nanopore
Circulating tumor DNA
Locked nucleic acid

ABSTRACT

Circulating tumor DNA (ctDNA), carrying tumor-specific sequence mutations, is a promising biomarker for classification, diagnosis and prognosis of cancers. However, there is still a great challenge in discriminating single-base difference between ctDNA and its coexisting analogue (normal circulating DNA, ncDNA) at a serum sample. A locked nucleic acid (LNA) probe combined with α-HL nanopore sensor was designed, which achieved a high signal-to-background ratio (SBR) of $\sim 8.34 \times 10^3$, as well as a significant discrimination capability ($\sim$12.3 times) of single-base difference. The accurate discrimination strategy is label-free, convenient, selective and sensitive, which has great potential in the early diagnosis of diseases and biomedical research fields.

Circulating tumor DNA (ctDNA), carrying tumor-specific sequence mutations, is a promising biomarker for classification, diagnosis and prognosis of cancers [1–3]. Detection of ctDNA is attracting much attention because its level in the peripheral blood has been associated with tumor burden and malignant progression. However, it is still a great challenge to achieve the selective detection in the peripheral blood because ctDNA, composed of small nucleic acid fragments, generally represents a small fraction (< 1.0%) of the total cell-free DNA (cfDNA) whilst its analogue with single base substitutions coexists (normal circulating DNA, ncDNA) [4,5]. In addition, single-stranded ctDNAs have a short half-life which is less than 2 h in blood [6]. Some ctDNA sensors have been proposed, such as a nanoplasmonic strategy based on peptide nucleic acids (PNAs) [7] and a DNA-mediated surface-enhanced Raman scattering (SERS) sensor [8]. Besides polymerase chain reaction (PCR) [2], all these technologies have led to significant contributions to ctDNA detection, but further application is still hindered by complex sample preparation, tedious labeling procedures and experimental skills [4,9]. Especially, these single-signal response strategies are incapable of simultaneously discriminating ctDNA with single-base difference.

Nanopore-based sensors, with the size-selective properties, have become a new class of single-molecule analytical technology [10–14]. The classical nanopore is bacterial protein α-hemolysin (α-HL) that can self-assemble across a planar lipid bilayer and form a transmembrane nanopore with the diameter of $\sim$1.4 nm [15–17]. Based on characteristic dwell time, α-HL nanopore sensors have been explored to specifically detect disease-DNA/RNA biomarker even with single-base mismatch [18–23]. Gu *et al.* proposed a polycationic peptide-peptide nucleic acid probe for detecting microRNAs with a 150-fold dwell time difference [20]. Our group reported a shared-arm molecular beacon (MB) used as a specific probe. Compared to common linear probe or classic MB, the shared-arm MB achieved an enhanced signal-to-background ratio (SBR) of $\sim 10^4$, higher thermodynamic stability to bind with target sequence, and faster hybridization rate [21]. The α-HL nanopore based on shared-arm MB simultaneously discriminated full-matched target DNA and single-base mismatch with a 6-fold dwell time difference.

Recently, locked nucleic acid (LNA) was explored to be a nanopore probe because LNA/DNA hybridization have increased helical thermostability (higher melting temperature, T_m) compared with DNA/DNA [24,25]. The LNA introduced in mismatch site (such as A-T and A-G) can cause a dramatically magnified melting temperature difference (ΔT_m) from 4.9 °C to 10.5 °C between the full-matched and single-base mismatched hybrid duplexes. It is because LNA has a methylene bridge that connects the 2′-oxygen of ribose with the 4′-carbon [26–28].

This covalent bridge effectively 'locks' the ribose in the N-type conformation that is dominant in A-form DNA [29]. The other

* Corresponding author.
E-mail address: zcs@scu.edu.cn (C. Zhou).

https://doi.org/10.1016/j.cclet.2019.05.033

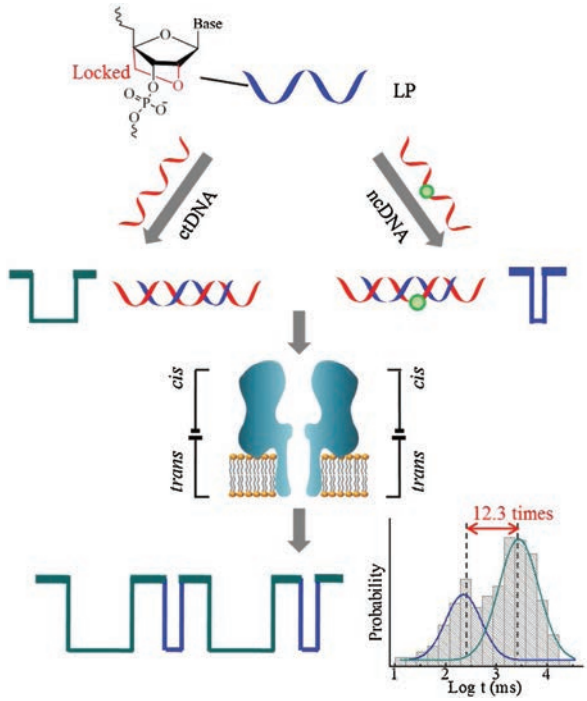

Fig. 1. Illustration of LNA probe (LP)-enabled discrimination of ctDNA and ncDNA in a nanopore.

reason is that LNA possesses a favorable toxicity profile [30,31] and a relative degree of nuclease resistance [32,33]. Gu *et al.* reported a single LNA approach that enhanced the DNA single-nucleotide polymorphism (SNP) discrimination capability by over 22-fold unzipping time difference [22]. Wang *et al.* reported that a LNA probe enabled a discrimination of microRNA with single nucleotide mismatch [23]. Although some kinds of probes listed above have made contributions to the specific discrimination, there are no reports on the simultaneous discrimination of ctDNA with single-nucleotide difference.

In this work, we designed a LNA probe for the α-HL nanopore to simultaneously discriminate ctDNA and ncDNA with single-base difference (Fig. 1). A single-stranded fragment KRAS G12DM [34], which expression level was associated with colon carcinoma, was chosen as the model ctDNA. LNA probe with the optimized length of 11 nucleotides, preformed the significant ΔT_m between full-matched and single-base mismatched duplexes, and greatly improved the discrimination capability of single-base mismatch up to ~12.3 times. The designed LNA probe achieved simultaneous identification of ctDNA and similar sequence ncDNA in a serum sample. The designed LNA-based nanopore sensor is label-free and highly specific for discriminating ctDNA with single-base difference, which has potential applications in early diagnosis and prognosis of tumors.

Firstly, we explored the feasibility of the designed LNA probe for detecting ctDNA. The 15-nt ctDNA from KRAS G12DM gene [34], a promising biomarker of colon carcinoma was used as the model target, and a LNA probe (LP) was designed to enhance the specific hybridization capability. The materials and the investigation methods used in this work were presented in Supporting information. This probe was extended at the 3′ end with a sequence of poly(dA)$_{13}$ that acted as a guide to lead the LP/ctDNA hybrids enter the vestibule of the nanopore for subsequent translocation and increase the frequency of translocation events. The voltage-dependent experiments confirmed that the mean dwell time of translocation behavior decreased as transmembrane potential increased (Fig. S1 in Supporting information). In order to test the recognition capability of LP for ctDNA, we analyzed the translocation events of all analytes, including ctDNA, LP, and the

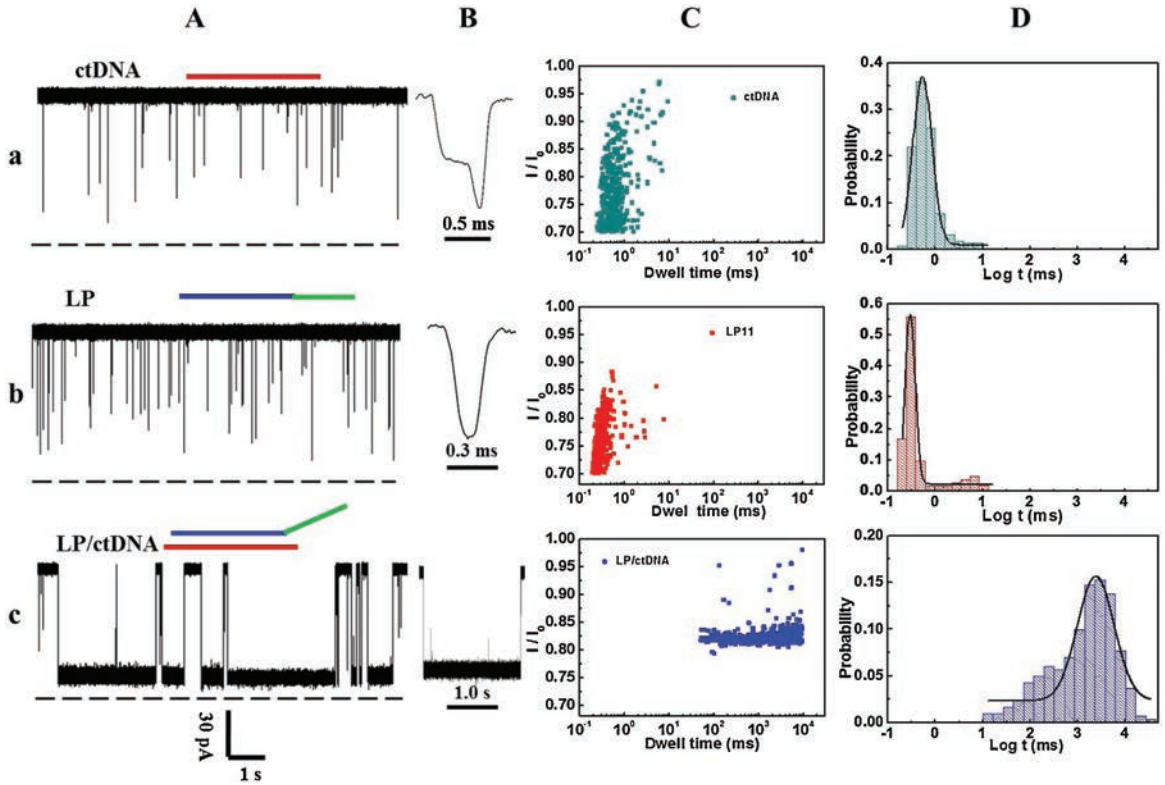

Fig. 2. Detection profile of ctDNA with a LNA probe. (A, B) Representative single-channel current traces of ctDNA (a), LP (b) and LP/ctDNA (c); (C) Scattering plots and (D) histograms of dwell time for ctDNA, LP and LP/ctDNA.

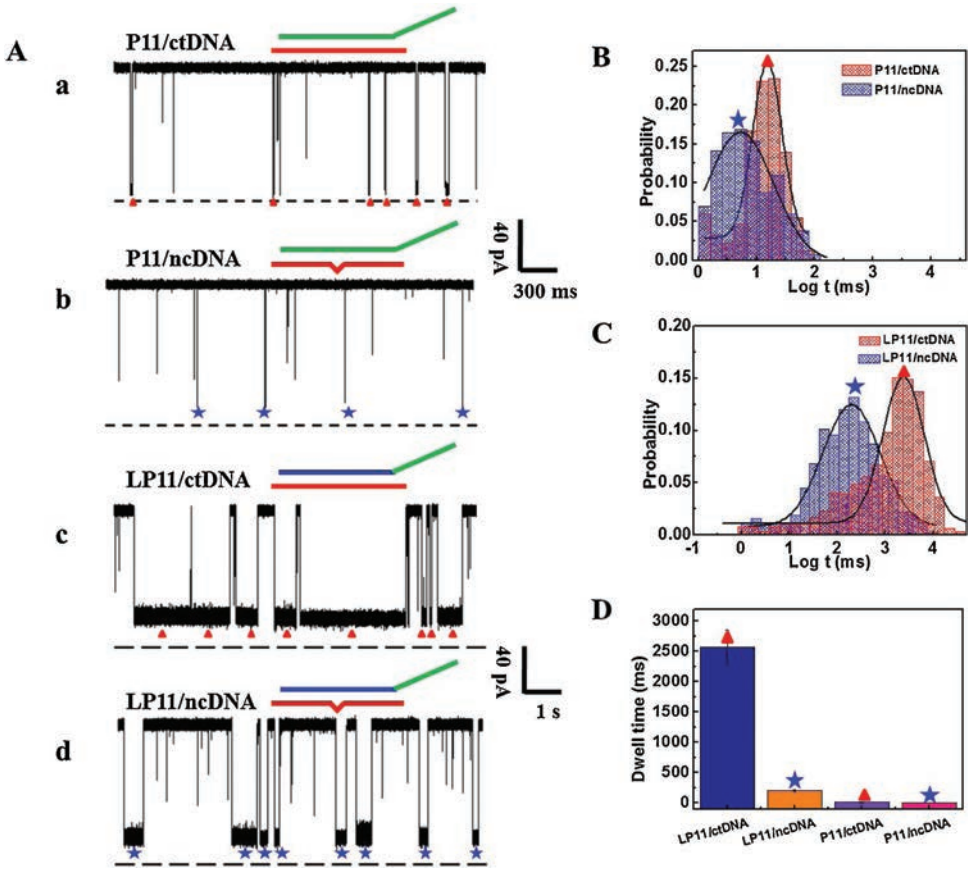

Fig. 3. Discrimination of ctDNA and ncDNA using P11 and LP11 probes. (A) Representative single-channel current traces for the test of the P11/ctDNA (a), P11/ncDNA (b), LP11/ctDNA (c) and LP11/ncDNA (d); Histograms of dwell time for two hybrids using P11 (B) and LP11 probes (C); (D) Comparison of dwell time of the four hybrids using P11 and LP11 probes.

hybrid added into the *cis* side of the nanopore at an applied potential of +140 mV. As shown in Fig. 2, the addition of ctDNA and LP produced translocation events with mean dwell time of 0.58 ± 0.06 ms and 0.30 ± 0.01 ms, respectively (Fig. 2D-a and D-b). LP and ctDNA were mixed and prehybridized at the room temperature. Translocation events of the mixture showed remarkably long blocks that lasted for 2502.93 ± 287.43 ms (Fig. 2D-c), $\sim 6.82 \times 10^3$ and $\sim 8.34 \times 10^3$ longer than that of ctDNA and LP alone, respectively (Fig. S2 in Supporting information). It was demonstrated that LP can strongly bind with ctDNA. The LNA-based nanopore sensor performed a high SBR of $\sim 8.34 \times 10^3$, ~400-fold higher than that of fluorescence-labeled strategies for sensing the ctDNA target [35]. It was also higher than the SBR of other LNA-based nanopore sensors for detecting disease-associated microRNA ($\sim 6.55 \times 10^3$) [23] and for sensing foodborne pathogenic DNA biomarker ($\sim 6.10 \times 10^2$) [22]. The LP probe, having such a high SBR, provides great potential for accurately sensing ctDNA.

Then, we investigated whether LNA could enhance the discrimination capability of ctDNA and ncDNA. As a coexisting analogue of ctDNA in the peripheral blood, ncDNA has only single-base substitution. The single nucleotide polymorphism site is located in the middle of the ctDNA sequence, which is a thymine (T) in the ctDNA and a cytosine (C) in ncDNA. To achieve the accurate discrimination of ctDNA and ncDNA, a series of LNA probes with different sequence lengths were designed (Table S1 in Supporting information). We valued ΔT_m between LP/ctDNA hybrid and LP/ncDNA hybrids through mfold Web Server [36], where LP was replaced by DNA probe. The comparison results (Table S2 in Supporting information) showed that the LP11 performed the largest ΔT_m, that suggested that the LP11/ctDNA hybrid have the highest thermostability compared with other hybrids.

The α-HL nanopore sensor was used to monitor translocation behaviors of the hybrid P11/ctDNA, P11/ncDNA, LP11/ctDNA and LP11/ncDNA at +140 mV (Fig. 3A). When DNA probe (P11) was used, the full-matched P11/ctDNA generated numerous blocks with an average dwell time of 9.66 ± 1.15 ms, while the single-base mismatched P11/ncDNA hybrid performed a dwell time of 4.91 ± 0.97 ms. The discrimination capability of the P11 probe was ~2.0 times (Fig. 3B). For the LNA probe, the dwell time of the full-matched LP11/ctDNA and mismatched LP11/ncDNA was increased to 2502.93 ± 287.43 ms and 204.06 ± 20.76 ms, respectively. The discrimination capability of LP11 was enhanced by ~12.3-fold (Fig. 3C). This was consistent with the ΔT_m results listed above. Furthermore, the results in Fig. 3D indicated that the combination of the LNA with the nanopore technology possesses an enhanced specificity in discriminating a single-nucleotide difference between ctDNA and ncDNA.

In order to figure out the enhanced discrimination capability of LP11 probe, we further analyzed the translocation frequencies (f) produced by DNA probe or LNA probe (Table S3 in Supporting information). For DNA probe, the translocation frequencies of full match (P11/ctDNA) and single-base mismatch (P11/ncDNA) were almost the same, $32.16 \pm 10.69\ min^{-1}$ and $33.75 \pm 4.03\ min^{-1}$, respectively. Significantly, the translocation frequency of full-matched LP11/ctDNA was increased to $47.62 \pm 6.60\ min^{-1}$. It is supported by previous reports that LNA molecule has a covalent methylene bridge that makes A-form helical structure dominant [24].

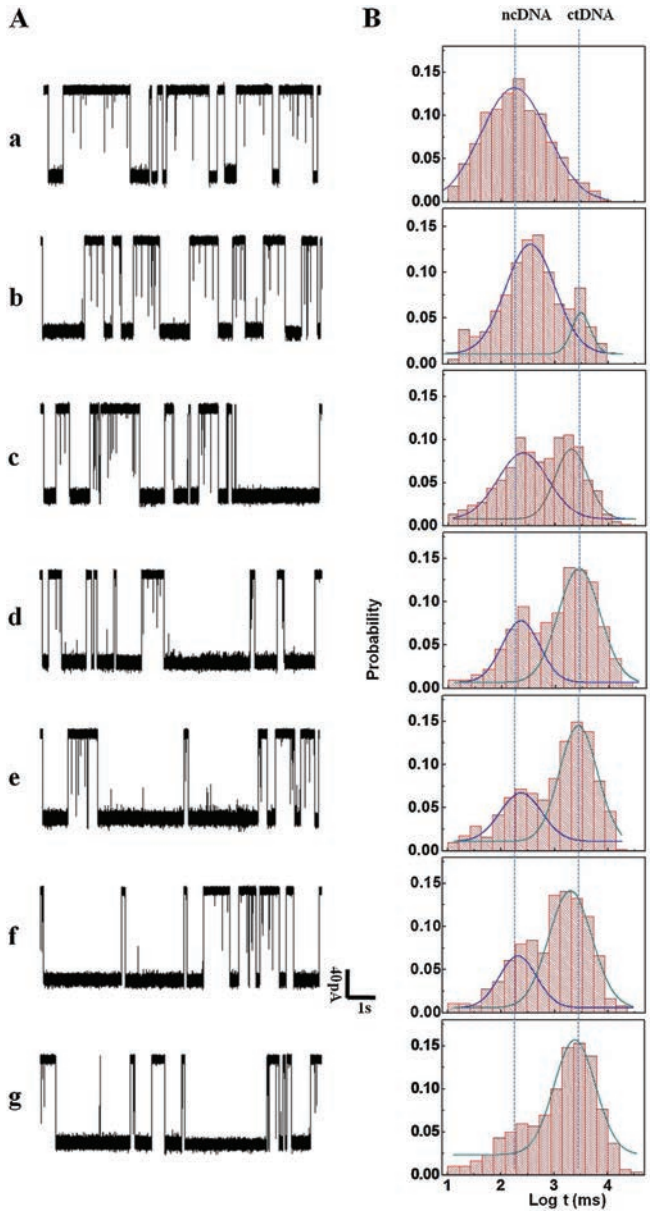

Fig. 4. Specific discrimination of ctDNA from a mixture solution using LP11 probe. (A) Current traces and (B) histograms of dwell time of mixture of LP11 with ncDNA and ctDNA at different concentration ratios: (a–g) ncDNA:ctDNA = 200:0, 180:20, 150:50, 100:100, 50:150, 20:180, 0:200. The total concentration of ncDNA and ctDNA was 200 nmol/L.

To further explore the simultaneous discrimination of single-nucleotide difference in the LP11 probe, translocation behaviors of various mixtures were recorded at the applied potential of +140 mV (Fig. 4). As shown in Fig. 4B, for the LP11/ctDNA alone, one peak of blockage with a mean dwell time of 2502.93 ± 287.43 ms was observed, while the LP11/ncDNA alone had the mean dwell time of 204.06 ± 20.76 ms. Subsequently, a series of mixture solutions containing various concentration ratios of ctDNA to ncDNA were tested through the LNA-based nanopore sensor. Two characteristic and well-separated dwell time peaks were observed. When the concentration of ctDNA was as low as 20 nmol/L, 9 times lower than that of ncDNA, LP11 can discriminate it from its coexistence ncDNA. The relative peak area of LP11/ctDNA was gradually enhanced as the concentration ratio of ctDNA to ncDNA increased. The peak area ratios of ctDNA over ncDNA were 0.14, 0.69, 2.07, 2.16 and 2.61, corresponding to mixture samples 20:180, 50:150, 100:100, 150:50 and 180:20, respectively, which demonstrated that ctDNA and ncDNA were simultaneously discriminated quite well. As far as we know, it is the first report on ctDNA-related simultaneous discrimination. In this work, on the basis of two characteristic and well-separated dwell time peaks, LP11 can work as a potential molecular tool for simultaneously discriminating ctDNA from mismatched ncDNA, which is expected to be used for early diagnosis and screening of tumors.

To evaluate the application of the LNA-based nanopore strategy in detecting ctDNA in real biological samples, ctDNA was directly spiked into the normal human serum samples (10%, v/v). As shown in Fig. S3 (Supporting information), the current traces of the serum samples retained a low level of noise-like spikes, similar to the results reported in the literature [23]. However, for the mixture of the serum samples with LP11, a large number of spike-like short blocks were recorded, corresponding to the characteristic dwell time of LP11. At the presence of ctDNA and LP11 in the serum samples, plenty of long blocks corresponding to LP11/ctDNA were recorded. Although ctDNA and ncDNA coexisted in the serum samples with a low concentration ratio of 20:180, the characteristic dwell time peak of ctDNA was easily discriminated from that of ncDNA. It was demonstrated that the LNA-based nanopore sensor can be used to specifically detect ctDNA in human serum samples.

For the Gaussian distribution overlap between LP11/ctDNA and LP11/ncDNA, the receiver operating characteristic (ROC) curve analysis was used to evaluate the accuracy of discrimination capability. The ROC has been a widely accepted diagnostic tool that measures the accuracy of a test to discriminate true positive events from false positive ones [18,22]. For each of the selected dwell time thresholds, there would be some true positive (TP = 0-1) and false positive (FP = 0-1) events. The area under the ROC curve (AUC) (0.5-1) indicated the accuracy of the method for discriminating single-nucleotide difference. ROC was analyzed using web-based calculator [37]. As shown in Fig. S4 (Supporting information), the AUC generated by P11 was only 0.60, and surprisingly the AUC was increased to 0.82 when LP11 was used. According to the reported evaluation criteria, the AUC of 0.82 indicates that the single-nucleotide difference discrimination accuracy for ctDNA and ncDNA can be evaluated as "good". That means that the translocation events presented in the overlap range can be evaluated as ctDNA with the true positive fraction of 82%. In addition, its good anti-interference capability was also confirmed since all results in serum samples were similar to the records in non-serum samples (Figs. S5 and S6 in Supporting information).

In summary, a LNA probe was designed to simultaneously discriminate ctDNA and its coexisting analogue (ncDNA) in a nanopore. The single-stranded fragment KRAS G12DM used as the model ctDNA, the designed LNA probe performed a high signal-to-background ratio of $\sim 8.34 \times 10^3$ for sensing target ctDNA based on nanopore electronic signals. Based on the enhanced thermostability (T_m) of the LNA/ctDNA hybrid, the discrimination capability of the LNA probe for ctDNA and ncDNA in a serum sample reached up to ~12.3 times. This simultaneous discrimination strategy is label-free, convenient, selective, and sensitive, which has great potential in the early diagnosis of diseases and biomedical research fields.

Acknowledgments

This work was financially supported by the National Natural Science Foundation of China (Nos. 21475091, 21775106). We greatly thank Prof. Long's group for establishing the experimental protocols, and providing the data analysis software.

Appendix A. Supplementary data

Supplementary data associated with this article can be found, in the online version, at https://doi.org/10.1016/j.cclet.2019.05.033.

References

[1] F.C. Bidard, B. Weigelt, J.S. Reis-Filho, Sci. Transl. Med. 5 (2013) 207ps14.
[2] A.M. Newman, S.V. Bratman, J. To, et al., Nat. Med. 20 (2014) 548–554.
[3] F. Cheng, L. Su, C. Qian, Oncotarget 7 (2016) 48832–48841.
[4] L.A. Diaz Jr., A. Bardelli, J. Clin. Oncol. 32 (2014) 579–586.
[5] H. Schwarzenbach, D.S.B. Hoon, K. Pantel, Nat. Rev. Cancer 11 (2011) 426–437.
[6] F. Diehl, K. Schmidt, M.A. Choti, Nat. Med. 14 (2008) 985–990.
[7] A.H. Nguyen, S.J. Sim, Biosens. Bioelectron. 67 (2015) 443–449.
[8] Q. Zhou, J. Zheng, Z. Qing, et al., Anal. Chem. 88 (2016) 4759–4765.
[9] M. Murtaza, S.J. Dawson, D.W.Y. Tsui, et al., Nature 497 (2013) 108–112.
[10] C. Cao, Y.L. Ying, Z.L. Hu, et al., Nat. Nanotech. 11 (2016) 713–718.
[11] Y.L. Ying, Y.T. Long, Sci. China Chem. 60 (2017) 1187–1190.
[12] C. Qi, J. Ding, B. Yuan, Y. Feng, Chin. Chem. Lett. 30 (2019) 1618–1626.
[13] H. Cai, C. Zhou, Q. Yang, et al., Chin. Chem. Lett. 29 (2018) 531–534.
[14] S. Rauf, L. Zhang, A. Ali, Y. Liu, J. Li, ACS Sens. 2 (2017) 227–234.
[15] L. Song, M.R. Hobaugh, C. Shustak, et al., Science 274 (1996) 1859–1865.
[16] Y.L. Ying, J. Zhang, R. Gao, Y.T. Long, Angew. Chem. Int. Ed. 52 (2013) 13154–13161.
[17] Q. Jin, A.M. Fleming, C.J. Burrows, H.S. White, J. Am. Chem. Soc. 134 (2012) 11006–11011.
[18] Y. Wang, D. Zheng, Q. Tan, M.X. Wang, L.Q. Gu, Nat. Nanotech. 6 (2011) 668–674.
[19] F. Yao, Y. Zhang, Y. Wei, X. Kang, Chem. Commun. (Camb.) 50 (2014) 13853–13856.
[20] K. Tian, Z. He, Y. Wang, S.J. Chen, L.Q. Gu, ACS Nano 7 (2013) 3962–3969.
[21] Q. Yang, T. Ai, Y. Lv, et al., Anal. Chem. 90 (2018) 8102–8107.
[22] K. Tian, X. Chen, B. Luan, et al., ACS Nano 12 (2018) 4194–4205.
[23] D. Xi, J. Shang, E. Fan, et al., Anal. Chem. 88 (2016) 10540–10546.
[24] Y. You, B.G. Moreira, M.A. Behlke, R. Owczarzy, Nucleic Acids Res. 34 (2006) e60.
[25] T. Natsume, Y. Ishikawa, K. Dedachi, T. Tsukamoto, N. Kurita, Chem. Phys. Lett. 446 (2007) 151–158.
[26] C. Wahlestedt, P. Salmi, L. Good, et al., Proc. Natl. Acad. Sci. U. S. A. 97 (2000) 5633–5638.
[27] A. Ciesielska, D.H. Mathews, D.H. Turner, et al., Nucleic Acids Res. 33 (2005) 5082–5093.
[28] A.A. Koshkin, S.K. Singh, P. Nielsen, et al., Tetrahedron 54 (1998) 3607–3630.
[29] M. Petersen, K. Bondensgaard, J. Wengel, J.P. Jacobsen, J. Am. Chem. Soc. 124 (2002) 5974–5982.
[30] B. Vester, J. Wengel, Biochemistry 43 (2004) 13233–13241.
[31] E.M. Straarup, N. Fisker, M. Hedtjärn, et al., Nucleic Acids Res. 38 (2010) 7100–7111.
[32] H.F. Hansen, T. Koch, Nucleos. Nucleot. Nucl. 22 (2003) 1041–1043.
[33] K.S. Schmidt, S. Borkowski, J. Kurreck, et al., Nucleic Acids Res. 32 (2004) 5757–5765.
[34] W. De Roock, B. Biesmans, J. De Schutter, Mol Diagn. Ther. 13 (2009) 103–114.
[35] Y. Chen, S.H. Lee, C. Mao, Angew. Chem. Int. Ed. 43 (2004) 5335–5338.
[36] http://unafold.rna.albany.edu/?q=DINAMelt/Hybrid2.
[37] http://www.rad.jhmi.edu/jeng/javarad/roc/JROCFITi.html.